

Automatic segmentation and quantification of the cardiac structures from non-contrast-enhanced cardiac CT scans

Shahzad, Rahil; Bos, Daniel; Budde, Ricardo P.J.; Pellikaan, Karlijn; Niessen, Wiro J.; Van Der Lugt, Aad; Van Walsum, Theo

DOI

[10.1088/1361-6560/aa63cb](https://doi.org/10.1088/1361-6560/aa63cb)

Publication date

2017

Document Version

Final published version

Published in

Physics in Medicine and Biology

Citation (APA)

Shahzad, R., Bos, D., Budde, R. P. J., Pellikaan, K., Niessen, W. J., Van Der Lugt, A., & Van Walsum, T. (2017). Automatic segmentation and quantification of the cardiac structures from non-contrast-enhanced cardiac CT scans. *Physics in Medicine and Biology*, 62(9), 3798-3813. <https://doi.org/10.1088/1361-6560/aa63cb>

Important note

To cite this publication, please use the final published version (if applicable).
Please check the document version above.

Copyright

Other than for strictly personal use, it is not permitted to download, forward or distribute the text or part of it, without the consent of the author(s) and/or copyright holder(s), unless the work is under an open content license such as Creative Commons.

Takedown policy

Please contact us and provide details if you believe this document breaches copyrights.
We will remove access to the work immediately and investigate your claim.

Automatic segmentation and quantification of the cardiac structures from non-contrast-enhanced cardiac CT scans

Rahil Shahzad^{1,2}, Daniel Bos^{3,4}, Ricardo P J Budde^{3,5},
Karlijn Pellikaan³, Wiro J Niessen^{2,6}, Aad van der Lugt³
and Theo van Walsum²

¹ Division of Image Processing, Department of Radiology, Leiden University Medical Center, 2300 RC Leiden, Netherlands

² Biomedical Imaging Group Rotterdam, Departments of Radiology & Nuclear Medicine and Medical Informatics, Erasmus MC—University Medical Center, 3015 GE Rotterdam, Netherlands

³ Department of Radiology & Nuclear Medicine, Erasmus MC—University Medical Center, 3015 GE Rotterdam, Netherlands

⁴ Department of Epidemiology, Erasmus MC—University Medical Center, 3015 GE Rotterdam, Netherlands

⁵ Department of Cardiology, Erasmus MC—University Medical Center, 3015 GE Rotterdam, Netherlands

⁶ Quantitative Imaging Group, Department of Imaging Physics, Delft University of Technology, 2628 CJ Delft, Netherlands

E-mail: r.shahzad@lumc.nl

Received 16 January 2017, revised 16 February 2017

Accepted for publication 1 March 2017

Published 11 April 2017



CrossMark

Abstract

Early structural changes to the heart, including the chambers and the coronary arteries, provide important information on pre-clinical heart disease like cardiac failure. Currently, contrast-enhanced cardiac computed tomography angiography (CCTA) is the preferred modality for the visualization of the cardiac chambers and the coronaries. In clinical practice not every patient undergoes a CCTA scan; many patients receive only a non-contrast-enhanced calcium scoring CT scan (CTCS), which has less radiation dose and does not require the administration of contrast agent. Quantifying cardiac structures in such images is challenging, as they lack the contrast present in CCTA scans. Such quantification would however be relevant, as it enables population based studies with only a CTCS scan. The purpose of this work is therefore to investigate the feasibility of automatic segmentation and quantification of cardiac structures viz whole heart, left atrium, left ventricle, right atrium, right ventricle and aortic root from CTCS scans. A fully automatic multi-

atlas-based segmentation approach is used to segment the cardiac structures. Results show that the segmentation overlap between the automatic method and that of the reference standard have a Dice similarity coefficient of 0.91 on average for the cardiac chambers. The mean surface-to-surface distance error over all the cardiac structures is 1.4 ± 1.7 mm. The automatically obtained cardiac chamber volumes using the CTCS scans have an excellent correlation when compared to the volumes in corresponding CCTA scans, a Pearson correlation coefficient (R) of 0.95 is obtained. Our fully automatic method enables large-scale assessment of cardiac structures on non-contrast-enhanced CT scans.

Keywords: multi-atlas-based segmentation, computed tomography, image registration, cardiac segmentation

(Some figures may appear in colour only in the online journal)

1. Introduction

Cardiovascular diseases remain the number one cause of death and disability worldwide (Mozaffarian *et al* 2016). Besides acute cardiovascular events such as stroke and myocardial infarctions, (chronic) heart failure is a rapidly growing global health problem (Lloyd-Jones *et al* 2002, Yancy *et al* 2013, Mozaffarian *et al* 2016). In addition to its considerable contribution to cardiovascular mortality, heart failure puts a substantial financial burden on healthcare systems (Robertson *et al* 2012). This highlights the urgent need for preventative strategies for heart failure (Schocken *et al* 2008). An essential step towards such strategies is the identification of early markers of the disease (D'Agostino *et al* 2008).

From an etiological point of view, many changes occur to the structure of the myocardium before heart failure may become clinically apparent (Heusch *et al* 2014). Interestingly, little is known about early, subtle changes in myocardial structure (remodelling) and whether or not these may be used as early predictive markers of heart failure.

One of the main imaging modalities used in cardiovascular disease is computed tomography (CT). As a result of rapid advances in processing techniques for cardiac imaging, quantification of cardiac structures has become possible. The quantified cardiac measures such as volumes of the atria and ventricles helps us assess the cardiac function, which is relevant for pre-clinical and clinical cardiovascular research (Kang *et al* 2012). Yet, quantification remains a tedious and time-consuming task when performed manually, which is not feasible in large studies or clinical practice.

Cardiac chamber segmentations are generally performed on cardiac CT angiography (CCTA) scans, due to the presence of contrast material that provides accurate identification of the different cardiac chambers. However, especially but not exclusively within the field of clinical cardiology, many patients undergo only a non-contrast-enhanced CT calcium scoring (CTCS) scan for various reasons (screening, planning, etc). In such cases, having a method that can accurately and robustly segment the cardiac structures on a CTCS scan with a similar precision as that on a CCTA scan will be of great clinical value. Information on cardiac structures may provide important additional insight into the risk of developing heart failure without additional testing or even without the use of contrast material. Also, having just one CT scan reduces both the radiation dose as well as the financial costs. Having a method that can automatically segment the cardiac structures on non-contrast-enhanced CTCS scans would therefore be of great interest where subjects undergo only a CTCS scan and do not have a

corresponding CCTA scan; not only in clinical practice, but also in the context of population based and screening studies (Bild *et al* 2002, Ardehali *et al* 2007, Hofman *et al* 2013, Hoffmann *et al* 2016).

1.1. Related work

Several (semi-)automatic methods for the segmentation of cardiac chambers on CCTA scans, where contrast agent is administered to visualize the coronaries and the cardiac chambers, have been addressed by a number of papers (Lorenz and von Berg 2006, Ecabert *et al* 2008, Zheng *et al* 2008, Kirişli *et al* 2010). In all of these methods, the appearance of the cardiac structures is relevant for the segmentation process as a strong contrast between the cardiac muscle tissue and the blood pool allows accurate identification of the cardiac chambers.

Multi-atlas-based segmentation is a very popular technique and has a number of applications in the field of medical imaging. A survey paper from Iglesias and Sabuncu (2015) presents the background and a range of applications. Atlas-based approaches are convenient, as they only need a limited set of annotated data. However, these methods require a representative dataset; representative with respect to the variation in anatomy, and representative with respect to the imaging modality. Literature covers a wide range of methods that use atlas-based approaches for segmenting cardiac CT scans (İşgum *et al* 2009, van Rikxoort *et al* 2010, Zuluaga *et al* 2013, Zhuang *et al* 2015). Multi-atlas-based methods for the purpose of cardiac chamber segmentations have only been applied and tested on CCTA datasets.

The method proposed in this paper is based on multi-atlas-based segmentation. We used this method to segment CTCS scans using CCTA atlases, which actually involves inter-modal registration. Inter-modality/multi-modality registration has been attempted previously to segment cardiac structures from lower resolution (poor contrast) scans using a higher resolution scan (Tavard *et al* 2014, Haak *et al* 2015, Zhuang and Shen 2016), these studies mainly focus on ultrasound scans (US) or magnetic resonance imaging (MRI). However, the feasibility of segmenting non-contrast-enhanced CTCS data using higher resolution CCTA scans have not been previously investigated.

1.2. Contributions

The purpose of this work is to develop and evaluate a fully automatic segmentation framework that can accurately and robustly segment the whole heart (WH), aortic root (AO), left ventricle (LV), left atrium (LA), right atrium (RA) and, right ventricle (RV) from CTCS scans. The segmented ventricles include both the blood-pool and the myocardial tissue. Thus, the quantified ventricular volumes are epicardial volumes. The work presented in this paper is built upon our previous works (Kirişli *et al* 2010, Shahzad *et al* 2013).

We previously presented and thoroughly evaluated a multi-atlas-based CCTA segmentation approach (Kirişli *et al* 2010), and have also evaluated to what extent this approach can be used to segment the whole heart in CTCS scans in the context of epicardial fat quantification (Shahzad *et al* 2013). In this study we assess the feasibility of segmenting the individual cardiac structures on non-contrast-enhanced CTCS scans. A very extensive validation is conducted, the performance of the proposed framework is assessed by: (i) comparing the contour surface-to-surface distances and Dice similarity coefficient for the cardiac structures on the CTCS scans between the automatic method and reference standard obtained from CCTA and CTCS scans, (ii) comparing the automatically obtained volumes of the cardiac structures from CTCS scans to those obtained semi-automatically using the CCTA scan and, (iii) comparing the segmentation accuracy of the cardiac structures obtained manually on a subset of 25 CTCS scans to the corresponding reference standard.

To the best of our knowledge this is the first study where a fully automatic approach for segmenting the cardiac chambers from CTCS scans has been presented and validated.

2. Materials and methods

2.1. Study population

For this study we retrospectively and randomly selected 100 subjects who have undergone a multi-detector computed tomography (MDCT) scan of the heart. The scans were acquired at Erasmus MC (Rotterdam, The Netherlands) using a Siemens Sensation 64 CT scanner (Siemens Medical Solutions, Forchheim, Germany).

The subjects were aged between 25–79 (mean age 58 ± 12) years old, 71% of the subjects were male. Each of these subjects underwent both a CTCS scan and CCTA scan. The scans were acquired for clinical diagnosis, and exhibit various pathologies. The cardiac scan ranged from the apex of the heart to the tracheal bifurcation. Both the CTCS and CCTA scans were acquired using ECG gating, using an absolute RR-interval time between -450 and -300 ms. The CTCS scans had an average in-plane pixel size of 0.35×0.35 , a slice thickness of 3 mm and a slice spacing of either 1.5 mm or 3 mm, the images were reconstructed using a b35f kernel. The CCTA scans had an average in-plane pixel size of 0.32×0.32 , a slice thickness of 0.75 mm and a slice spacing of 0.4 mm, the images were reconstructed using a b30f kernel. A tube voltage of 120 kV was used for both scan types.

From the initial dataset of 100 subjects, we excluded ten subjects; two subjects had extreme imaging artefacts caused due to metal implants and eight subjects had a cardiac phase mismatch between the CTCS and CCTA acquisition. The evaluation was thus performed on 90 datasets.

2.2. Method overview

The method proposed in this paper is based on a multi-atlas-based segmentation approach, as described in the work of Kirişli *et al* (2010). In the present work we use eight manually delineated CCTA scans as atlases to segment an unseen CTCS dataset. The reason for using the CCTA atlases is two-fold: first, these have been evaluated in a large CCTA segmentation study, and second, the presence of contrast agent allows for accurate delineation of the cardiac chambers. Figure 1 shows one of the eight annotated CCTA atlas scan.

The atlas building as well as the registration approach are discussed in the original work (Kirişli *et al* 2010), but for completeness we briefly explain the segmentation work-flow. Multi-atlas-based segmentation is a process where multiple atlas scans with corresponding manually annotated labels are registered to an unseen subject's scan (Rohlfing *et al* 2005). Image registration is used to spatially align the atlas scans and the subject's scan (Aljabar *et al* 2009). In the registration procedure, the transformation parameters \mathbf{T} that minimizes the cost function \mathcal{C} between the fixed image (I_f) and the a moving image (I_m) are determined. The final segmentation of the structures on the subject's scan is obtained by fusing all the resulting transformed labels (Rohlfing *et al* 2004). A number of label fusion strategies are present in literature. In this work, we use majority voting to combine the label images (Lam and Suen 1997). For detailed information on medical image registration readers are referred to (Bankman 2000, Suri *et al* 2007).

Registration details for multi-atlas-based segmentation for the CTCS scans are as follows. A two stage registration approach was used, an affine transformation followed by a non-rigid B-spline transformation. Mutual information was used as similarity measure for the cost

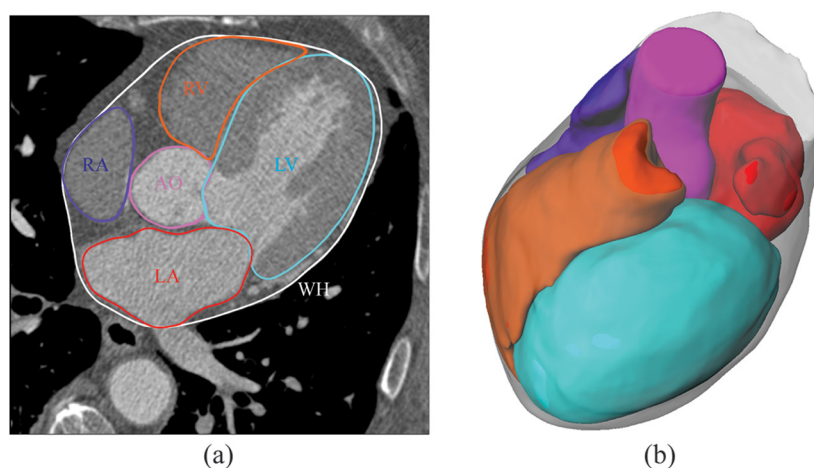


Figure 1. A CCTA atlas scan with the labelled cardiac structures on an axial slice (a). Label visualization in 3D (b).

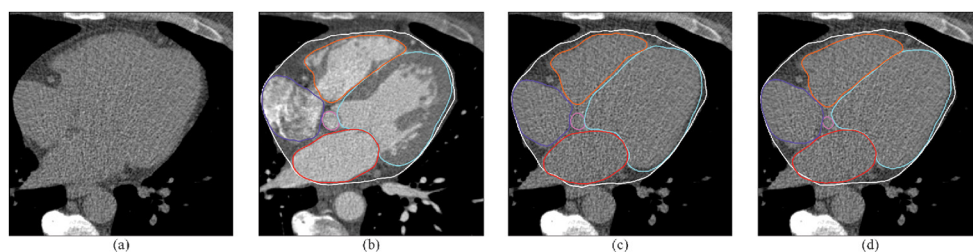


Figure 2. Image showing an axial slice of a random subject. CTCS scan before segmentation (a). The corresponding CCTA scan with the reference standard cardiac delineation (b). Result of the automatic cardiac segmentation on the CTCS scan (c). Reference standard CCTA cardiac delineation warped onto the CTCS scan (d).

function (Mattes *et al* 2003). Optimization was performed using adaptive stochastic gradient descent (Klein *et al* 2009). A three-stage multi-resolution coarse-to-fine scheme was used. The number of voxels sampled in each iteration was set at 1024, 2048 and 4096 for the affine transformation; 512, 1024 and 2048 for the B-spline transformation. The number of iterations was set to 512 for the affine transformation and 2048 for the B-spline transformation. Registrations were performed using *Elastix* a publicly available medical image registration software (Klein *et al* 2010).

The eight atlas transformed labels for each cardiac structure (*viz.* WH, AO, LV, LA, RA and, RV) were combined using majority voting. From the resulting segmented structures volumes (in ml) have been computed. Figure 2(a) shows a CTCS axial slice of a random subject, figure 2(c) shows the CTCS cardiac segmentations which were automatically obtained.

2.3. Reference standard

Reference standard segmentations were defined using both the CTCS and CCTA scans. Due to the CTCS imaging modality limitation (lower resolution and poor tissue contrast), it is not feasible to define a reliable reference standard using only these scans. A more practical approach of defining reference standard using both the CTCS and CCTA scans was used. As the CCTA

Table 1. Multi-atlas based segmentation quality check for cardiac structures on CCTA scans.

Grade	Description
I	Very accurate: Deviation up to 1 mm
II	Most structures accurate: 1 or 2 structures may deviate up to 3 mm
III	Most structures accurate: 1 structure may deviate up to 1 cm or more than 2 structures may deviate up to 3 mm
IV	A significant structure (up to 50%) has been incorrectly segmented
V	Segmentation failure

scans have a better resolution and higher tissue contrast, delineating the cardiac structures on these scans provides more accurate segmentations. In the following paragraphs we explain the process of defining the cardiac chamber segmentations on the CCTA scans and warping these segmentations onto the CTCS scans.

In this work we delineate the cardiac structures using a semi-automatic approach. An initial segmentation was obtained using the automatic approach (Kirişli *et al* 2010) and manual corrections were applied when necessary. For the manual correction, two experts (*DB*, *RB*) visually inspected the automatically obtained cardiac chamber segmentations on the 90 CCTA datasets. A grade was provided for each of the CCTA scan based on the quality of the segmentation, as defined in table 1. CCTA datasets which obtain grades I and II are considered to have good segmentations, as they generate very accurate volumetric measures for the cardiac structures. In the datasets that obtained grades III to V the segmentation errors were manually corrected by the clinical experts. Figure 2(b) shows the semi-automatically obtained CCTA cardiac structure segmentations for one of the subjects. 72 (80%) datasets were assigned to grade I, 7 to grade II, 9 to grade III and 2 obtained grade IV. None of the scans were assigned grade V.

Next, the CCTA segmentations were warped onto the CTCS scans. This is done by non-rigid registration of the subjects CCTA and CTCS scan. Subsequently, using this registration result, the CCTA segmentations were transformed to the CTCS image space to generate reference standard cardiac segmentations. Note that this registration, which is intra-subject, and performed on images that are acquired at the same scanning session and in the same cardiac phase, is quite straightforward, as there is not much motion or deformation to correct for. A simple affine registration between the inter-subject CCTA and CTCS scans could have been performed. But, for the sake of completeness and to compensate for any unforeseen patient motion an elastic registration was performed.

The intra-subject registration scheme was as follows. A two-stage approach and three-stage multi-resolution coarse-to-fine scheme similar to the multi-atlas registration was used. The major difference in the parameters is the number of iterations. Affine transformation had 256 iterations and B-spline transformation had 512 iterations. Figure 2(d) shows an example of the warped segmentations (from figure 2(b)) onto the CTCS scan.

To additionally evaluate the accuracy of the automatic method compared to manual segmentation, the cardiac structures on 25 randomly selected CTCS scans were manually delineated by an experienced medical student. The student received training from a radiologist. Once the manual annotations were completed, one of the experts (*DB*) analysed all the segmentations for accuracy and corrected them when necessary.

An in-house tool was used for manual delineation of the cardiac structures. The tool was developed using MeVisLab (MeVis Medical Solutions AG, Bremen, Germany). The observer delineated the cardiac structures using only the axial slices of the CTCS scans. The contour for the structure of interest was annotated by clicking a number of points along the structure and fitting a spline through the points. The observer had the possibility to adjust the window level settings for better visualization of the different tissue types. The observer also had the possibility to view the scans in a coronal or a sagittal view, facilitating a consistent segmentation over the slices.

2.4. Evaluation measures

To evaluate the accuracy of the automatically obtained CTCS cardiac segmentations four evaluation measures were used; (i) Visual inspection of the CTCS segmented results; (ii) Comparing the automatic CTCS chamber segmentations to the corresponding CTCS reference segmentations; (iii) Comparing the CTCS obtained cardiac volumes to the CCTA cardiac volumes; (iv) Comparing the reference standard cardiac segmentations to those obtained manually on CTCS scans.

To assess the quality of the segmentation results the experts visually inspected all the CTCS scans in 3D. Based on the accuracy of the cardiac chamber segmentations the scans were assigned one of these ranks: *good*, *moderate* or *bad*. A segmented CTCS scan is considered to be *good* if all cardiac structures are accurately segmented. A segmented CTCS scan is considered to be *bad* if one or more cardiac structures are grossly under- or over-segmented. The intermediate scans that have minor segmentation errors are assigned to the *moderate* rank.

The segmentation regions on the CTCS scans were compared using Dice similarity coefficient (DSC) and surface-to-surface distances between the reference standard and automatic results. For volumetric correlations of the cardiac structures Pearson correlation coefficient (R) and Bland–Altman analysis were performed.

3. Results

3.1. Qualitative assessment of CTCS segmentation

Visual inspection of the automatic cardiac segmentations on the 90 CTCS scans resulted in, 48 scans (53%) being assigned to the rank *good*, 31 (34%) to *moderate* and 11 (12%) to *bad* (See figure 3 for examples).

3.2. Agreement between the automatic and reference standard segmentation

To evaluate the performance of the automatic method, each of the automatically segmented CTCS structures' volumes were compared to those of the reference standard by using Pearson correlation coefficient (R) and Bland–Altman analysis. Also, average absolute volumetric differences between the two were computed. An average R of 0.95 (range 0.90–0.99) was obtained over all the cardiac structures and, an average volumetric difference for the cardiac structures was 17.6 (range 2.3–42.2) ml. Figure 4 shows the correlation plots for the WH and RV structures.

The performance of the proposed automatic method was further evaluated by comparing the reference standard contours to those obtained automatically. It was observed that the average Dice similarity coefficient (DSC) for the different cardiac structures was 0.91. The mean surface-to-surface distance between the contours over all the structures was 1.43 ± 1.73 mm.

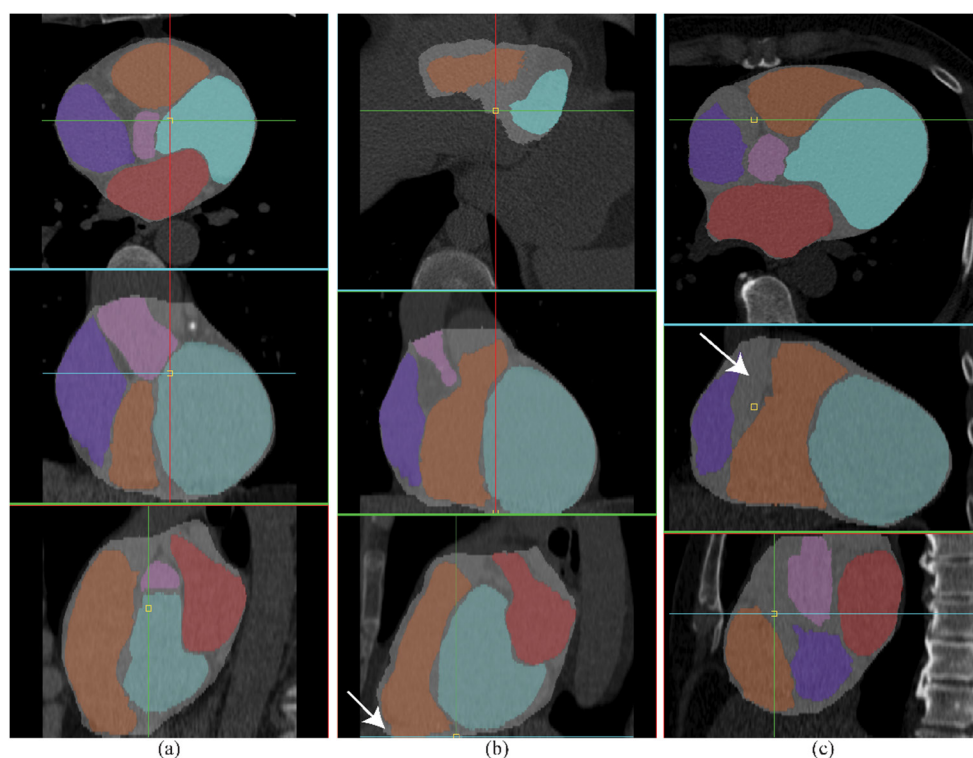


Figure 3. Axial, coronal and sagittal views of the cardiac segmentations used for qualitative assessment. A good quality segmentation (a). A moderate quality segmentation (b), where the RV and the WH are slightly overestimated on the last slice. A bad quality segmentation (c), where the RA is consistently under segmented. The white arrows indicate the location of the error on the most prominent view.

Figure 5 shows the boxplot of the DCS values for the different cardiac structures over all the subjects. Table 2 provides a complete list of all the quantified measures for each of the cardiac structure. It can be observed that the bias obtained from the Blant-Altman analysis for the WH and LV structures deviates away from zero and indicates that our method overestimates these volumes. To further investigate this bias a one sample t-Test was performed to assess whether volume differences of these two structures statistically significantly deviate from 0. The analysis indicated that the bias for these two structures is likely to arise from the method ($p < 0.001$ in both cases), however the magnitude of this error (Abs diff) is insignificant when compared to the average volumes of the structures.

3.3. Assessment of volumetric measurements between the automatic CTCS segmentation and the CCTA segmentation

To evaluate the accuracy with which the CTCS scans can be used to automatically segment the cardiac structures, volumes obtained from the automatic segmentations on CTCS scans and the CCTA manual segmentations were compared. The average Pearson correlation coefficient R over all the structures was 0.94. An average volumetric difference for the cardiac structures was 17.8 (range 2.8–38.6) ml. Table 3 provides the R measures for the individual structures. The Bland–Altman measures and the absolute volumetric difference are also provided.

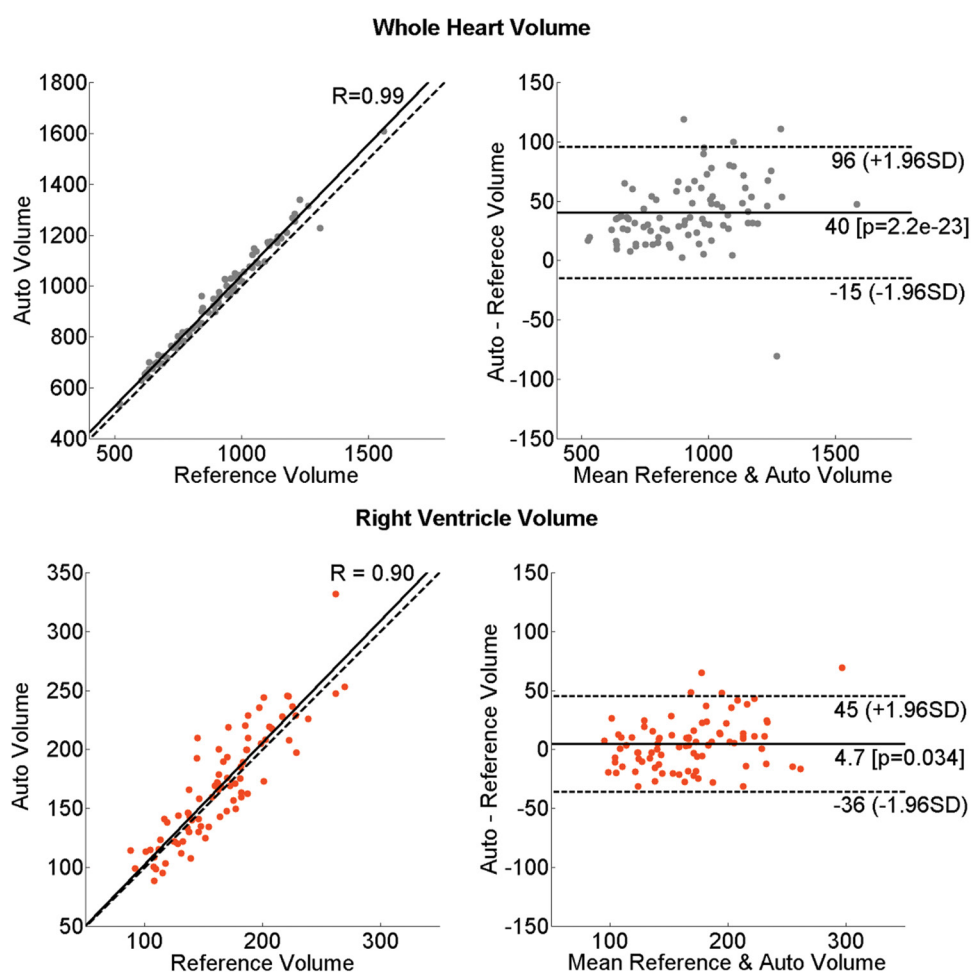


Figure 4. Correlation and Bland–Altman plots for the whole heart and right ventricle volumes. Comparison between the automatic segmentation and the reference volumes on the CTCS scans.

3.4. Performance of manual CTCS segmentations

The feasibility of cardiac chamber segmentations on the CTCS scans were measured by comparing manually obtained cardiac segmentations on the CTCS scans to the reference standard segmentation on a subset of 25 scans. It was observed that the R was 0.91 and average DSC was 0.85 for all the cardiac structures. For more detailed comparisons, the agreement between the automatically obtained segmentations and the reference standard segmentations for the same subset of 25 scans were also calculated. The obtained R was 0.95 and DSC was 0.91. Table 4 provides in-depth measures for the cardiac structures between the manual, automatic and the reference standard segmentations. Figure 6 presents the correlation plots for each of the cardiac structure. The correlation plots show both manual (in red) and automatic (in blue) volumetric comparisons.

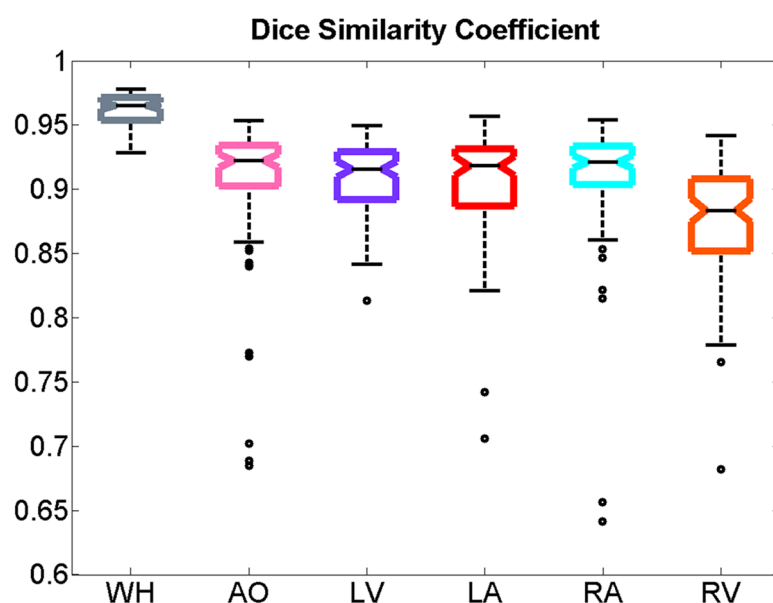


Figure 5. Boxplot representing the agreement between the automatic and reference CTCS segmentations. Values are represented as DSC.

4. Discussion

In this study, we presented and evaluated a fully automatic method for segmenting the individual cardiac structures using CTCS scans. The proposed method is based on a multi-atlas segmentation approach. We demonstrated that, using the atlas-based segmentation work-flow, cardiac chamber segmentations on CTCS scans can be automatically obtained to a precision similar to those from CCTA scan.

Comparing the automatically obtained cardiac chamber segmentations on the CTCS scans to the reference standard, it was observed that mean surface-to-surface distance (MSD) error was 1.43 ± 1.73 mm for the structures and the Dice similarity coefficient (DSC) was 0.91, which is close to the accuracy that we obtained in our previous study on the CCTA datasets where MSD was 1.26 ± 1.25 mm and DSC was 0.91. It should also be noted that the CTCS scans have a lower image resolution than that of the CCTA scan ($0.35 \times 0.35 \times 1.5$ mm versus $0.32 \times 0.32 \times 0.4$ mm). When the MSD on the CTCS scan is considered, the method proposed makes an error which is almost equal to a voxel in the axial direction. Figure 7 shows an example of the segmentation comparison. An average Pearson correlation coefficient (R) of 0.95 was obtained when the volumes of the segmented regions were compared, the highest correlation was obtained for WH (0.99) and the lowest for RV (0.90).

When the volumes of the cardiac chamber segmentations on the CTCS scans are compared to the CCTA scans, we see that the automatically obtained segmentations on the CTCS scans have good correlations to the semi-automatically obtained segmentations on the CCTA scans. A Pearson correlation coefficient (R) of 0.94 was obtained, Bland–Altman analysis showed that for most of the cardiac structure the bias is very small and the 95% confidence interval is not too large, which is also demonstrated by the absolute volume differences for each of the cardiac structure. On average, the absolute volume difference was 17.75 ml, the largest errors were made on the whole heart (WH) and the left ventricle (LV) structures which were 38.6 ± 31.0 ml and 34.2 ± 19.8 ml (see table 3). When these volumes are compared to the

Table 2. Comparison between the automatic method and the reference standard on CTCS scans. R is the Pearson correlation coefficient along with the linear regression β confidence interval (CI). B–A is the Bland–Altman bias along with the 95% CI. Abs diff is the average absolute difference. DSC is the dice similarity coefficient. MSD is the mean surface distance and MaxSD is the maximum surface distance. All volumes are represented in ml and distances in mm.

	WH	AO	LV	LA	RA	RV
Average volume						
Reference standard	895.8 ± 201.2	37.1 ± 11.5	278.9 ± 75.7	103.2 ± 31.1	87.1 ± 24.6	163.9 ± 40.1
Automatic method	936.2 ± 208.8	36.6 ± 10.5	307.5 ± 75.4	108.4 ± 31.2	89.8 ± 23.3	168.6 ± 46.3
Volumetric measures						
R	0.99	0.95	0.95	0.97	0.94	0.90
R (95% CI)	(0.99, 0.99)	(0.92, 0.96)	(0.93, 0.97)	(0.95, 0.98)	(0.91, 0.96)	(0.84, 0.93)
Bland–Altman (bias)	40	−0.37	29	5.2	2.8	4.7
Bland–Altman (95% CI)	(−15, 96)	(−8, 7)	(−17, 74)	(−11, 29)	(−14, −19)	(−36, 45)
Abs diff	42.2 ± 25.5	2.3 ± 2.9	31.3 ± 19.4	7.5 ± 5.6	6.1 ± 6.5	16.2 ± 13.6
Segmentation measures						
DSC	0.96	0.90	0.90	0.91	0.91	0.87
Sensitivity	0.98	0.90	0.96	0.89	0.89	0.86
Specificity	0.98	0.99	0.99	0.99	0.99	0.99
MSD	1.3 ± 1.8	1.0 ± 1.2	2.0 ± 2.3	1.2 ± 1.4	1.2 ± 1.5	1.9 ± 2.2
MaxSD	11.3 ± 4.8	6.3 ± 3.7	11.7 ± 3.6	8.4 ± 3.9	8.8 ± 3.9	12.0 ± 5.7

Table 3. Performance of the segmentations by comparing the automatic method to the CCTA segmentations. R is the Pearson correlation coefficient along with the linear regression β confidence interval (CI). B–A is the Bland–Altman bias along with the 95% CI. Abs diff is the average absolute volume difference. All volumes are represented in ml.

Structure	R (CI for β)	B–A (95% CI)	Abs diff
WH	0.99 (0.98, 0.99)	36 (−30, 100)	38.6 ± 31.0
AO	0.93 (0.90, 0.96)	0 (−8, 8)	2.8 ± 3.0
LV	0.95 (0.92, 0.96)	31 (−17, 79)	34.2 ± 19.8
LA	0.96 (0.94, 0.97)	6 (−11, 23)	8.6 ± 6.3
RA	0.91 (0.87, 0.94)	0 (−19, 20)	6.4 ± 7.6
RV	0.89 (0.84, 0.92)	3 (−39, 44)	15.9 ± 14.3

Table 4. Comparison between the automatic method and the manual segmentations to the reference standard on the 25 CTCS scans. A is automatic, R is reference and M is manual segmentations. DSC is the dice similarity coefficient. MSD is the mean surface distance and MaxSD is the maximum surface distance. R is the Pearson correlation coefficient along with the linear regression β confidence interval (CI). B–A is the Bland–Altman bias along with the 95% CI. Abs diff is the average absolute difference. All distances are in mm and volumes are represented as ml.

Cardiac Structure	R (CI for β)		B–A (95% CI)		Abs diff	
	A versus R	M versus R	A versus R	M versus R	A versus R	M versus R
WH	0.99 (0.98, 0.99)	0.97 (0.94, 0.99)	37 (–7, 81)	–45 (–120, 26)	37.76 \pm 20.72	47.11 \pm 33.92
AO	0.93 (0.85, 0.97)	0.86 (0.71, 0.94)	–1 (–11, 9)	1 (–15, 17)	2.95 \pm 4.15	5.63 \pm 5.93
LV	0.95 (0.88, 0.98)	0.94 (0.87, 0.98)	30 (–5, 66)	–7 (–43, 28)	30.24 \pm 18.11	17.27 \pm 8.82
LA	0.96 (0.91, 0.98)	0.87 (0.72, 0.94)	6 (–11, 23)	–26 (–54, 2)	8.60 \pm 5.57	27.48 \pm 11.91
RA	0.98 (0.95, 0.99)	0.95 (0.88, 0.98)	4 (–4, 12)	12 (–2, 27)	4.51 \pm 3.05	12.29 \pm 6.99
RV	0.88 (0.74, 0.94)	0.86 (0.71, 0.94)	4 (–31, 39)	32 (–16, 80)	13.37 \pm 12.14	32.76 \pm 23.61

Cardiac Structure	DSC		MSD		MaxSD	
	A versus R	M versus R	A versus R	M versus R	A versus R	M versus R
WH	0.96 \pm 0.01	0.92 \pm 0.02	1.22 \pm 0.39	2.31 \pm 0.63	10.75 \pm 2.60	17.45 \pm 3.40
AO	0.90 \pm 0.07	0.82 \pm 0.07	1.01 \pm 0.59	1.99 \pm 1.08	5.65 \pm 2.10	11.02 \pm 4.26
LV	0.92 \pm 0.03	0.89 \pm 0.02	1.89 \pm 0.71	1.97 \pm 0.51	10.28 \pm 2.41	14.17 \pm 2.56
LA	0.91 \pm 0.03	0.76 \pm 0.05	1.16 \pm 0.54	4.25 \pm 1.36	7.73 \pm 3.79	20.04 \pm 5.18
RA	0.91 \pm 0.03	0.88 \pm 0.03	1.09 \pm 0.43	1.80 \pm 0.53	8.38 \pm 2.42	14.09 \pm 4.58
RV	0.88 \pm 0.05	0.84 \pm 0.05	1.72 \pm 0.89	2.90 \pm 1.21	11.09 \pm 3.78	19.18 \pm 8.71

actual average size of the structures on the CCTA scans, the WH volume is about 900 ml and that for LV is 278 ml, thus the error made is around 4% and 10%, respectively. The average error made for the other structures is around 7% of their total volume.

We also evaluated the accuracy of manually delineated cardiac structures on a subset of 25 CTCS scans. We compared the results of the manual annotations and the automated quantification on CTCS scans to the reference standard. It was observed that the automatic method and the manual annotations were quite good when compared to the reference standard, with the automatic method having a slightly higher DSC. Detailed correlation plots for the volumetric measure are presented in figure 6. Closer inspection of the manual annotations showed that it was difficult for the human observer to distinguish between the atrium and the ventricle, a region where the multi-atlas-based method could perform much better as it uses both image intensity and cardiac structural information for the segmentation process. This resulted in a higher maximum surface-to-surface distance error for the manual segmentations when compared to the automatic method.

The backbone of our method is multi-atlas-based segmentation which requires image registration. Registration and transformation of the atlas scans and the subject's scan requires a bit of computation time. On a desktop PC (Intel Xenon CPU 3.60 GHz and 16 GB RAM) each of the atlas scans requires on average 1 min and 50 s of computation time. Thus, running of the entire framework on this desktop requires around 15 mins to segment all the cardiac structures from the scan. This time can be easily reduced by using more computational power: all eight atlas registrations can be run in parallel, thus even without code optimization, 2 min processing time is feasible in case a sufficiently large computational cluster is available.

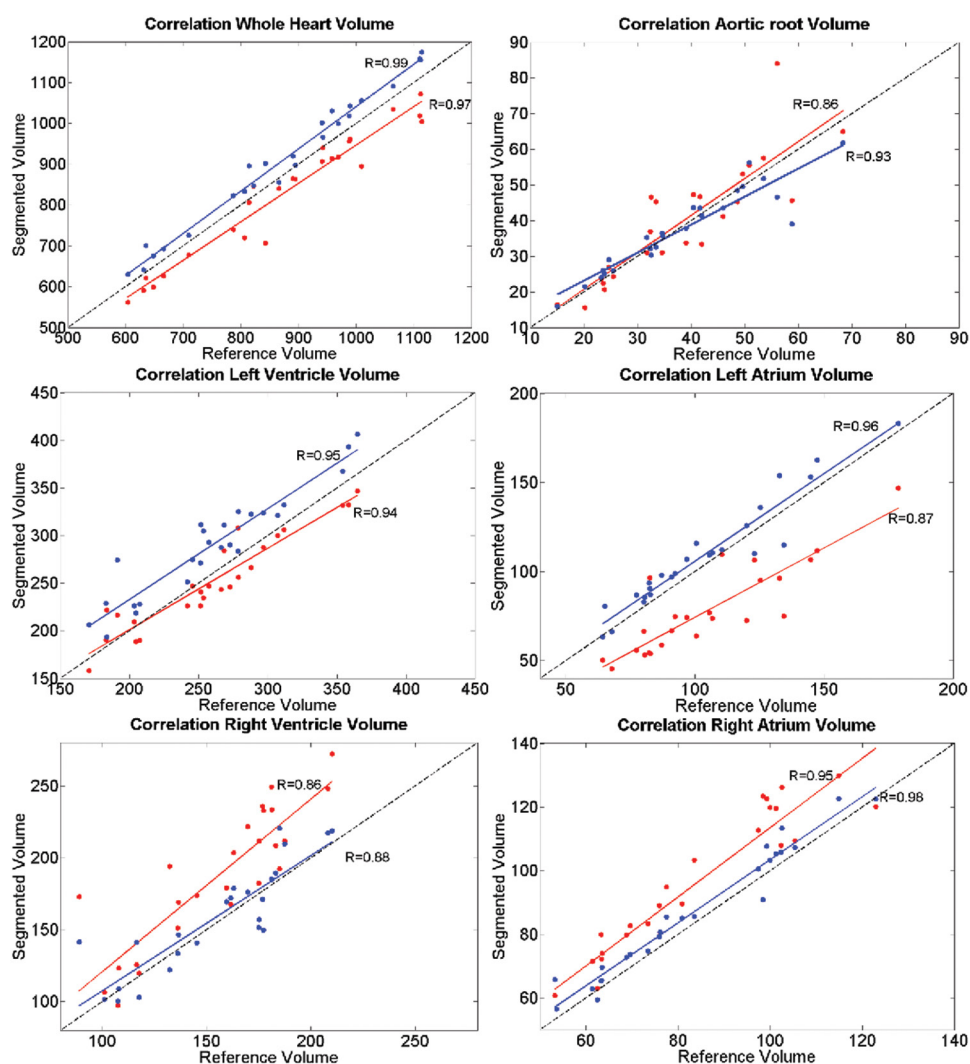


Figure 6. Correlation plots for the different cardiac structure volumes on the 25 CTCS scans. Correlation between the manual and the reference volumes is represented in red and that between the automatic and reference in blue.

Our method does have a few disadvantages. Figure 5, which shows the boxplot of the DCS values on the CTCS scans, shows a number of outliers (black circles), caused due to segmentation errors. These *bad* segmentations have also been reported in section 3.1, where 11 subjects had suboptimal segmentation results for one or more cardiac structures. It turns out that 6 out of the 11 subjects had issues with the automatic CCTA segmentations as well (section 2.3), and had to be manually corrected for. A closer inspection revealed that the majority of the segmentation errors occurred when the anatomy of the heart deviated from the ‘normal’ appearance. Multi-atlas-based segmentation could adopt to the change in anatomy up to a certain range but not beyond it. The main reason for this is that the eight CCTA scans used as atlases in our method do not cover all possible anatomical variations that can be clinically relevant. One possibility to improve the segmentation accuracy for subjects that have unusual cardiac anatomy would be to include more CCTA labelled atlas scans covering

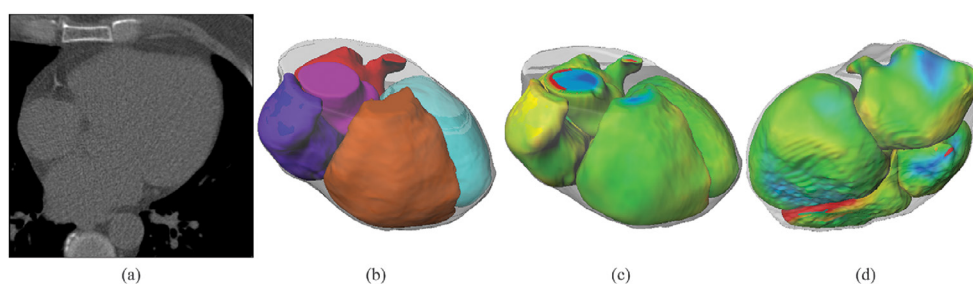


Figure 7. Segmentation results for one of the subjects. CTCS axial slice (a). Automatically obtained cardiac chamber segmentation (b). Automatic segmentation compared to reference standard from two angles ((c)–(d)). Colour map on images ((c)–(d)) represent surface-to-surface distance error rate, red indicates under-segmentation, blue indicates over-segmentation and yellow-green indicates good agreement.

a wider range of cardiac anatomy. Additional improvements can be achieved by using more advanced methods for atlas selection and label fusion strategies. Another drawback of the method is that the segmented LV also includes the surrounding myocardium. To obtain the clinically relevant LV volume, only the LV endocardium needs to be segmented. However, with the very poor contrast between the LV blood pool and the surrounding myocardial tissue on the CTCS scans our method is unable to distinguish the endocardium and the epicardium boundary accurately. Therefore, our method is only able to provide the epicardial LV volume.

We did not investigate the performance of our method on CTCS scans from multiple vendors. However, we are confident that the performance of our method would not deviate from the current results. Since the proposed method is built upon our previous study, where multi-vendor data was used to evaluate the segmentation accuracy on CCTA scans (Kirişli *et al* 2010), we believe that a similar accuracy would be obtained on CTCS scans from the other vendors.

5. Conclusion

An automatic method for segmenting the cardiac structures on non-contrast-enhanced CTCS scans was developed and extensively evaluated. We demonstrated that the proposed method has the ability to accurately segment the different cardiac structures on CTCS scans. The automatically obtained segmentations were as good as the ones obtained using contrast-enhanced CCTA scans. Thus demonstrating the ability to use the proposed method in large clinical or population studies to investigate the structure of the myocardium and other cardiac chambers where only CTCS scans are acquired.

Acknowledgments

The authors would like to acknowledge Hortense Kirişli and Coert Metz for their work on labelling the CCTA atlas scans.

References

- Aljabar P, Heckemann R A, Hammers A, Hajnal J V and Rueckert D 2009 Multi-atlas based segmentation of brain images: atlas selection and its effect on accuracy *Neuroimage* **46** 726–38

- Ardehali R, Nasir K, Kolandaivelu A, Budoff M J and Blumenthal R S 2007 Screening patients for subclinical atherosclerosis with non-contrast cardiac CT *Atherosclerosis* **192** 235–42
- Bankman I 2000 *Handbook of Medical Imaging: Processing and Analysis, Registration* (New York: Academic)
- Bild D E et al 2002 Multi-ethnic study of atherosclerosis: objectives and design *Am. J. Epidemiology* **156** 871–81
- D'Agostino R B, Vasan R S, Pencina M J, Wolf P A, Cobain M, Massaro J M and Kannel W B 2008 General cardiovascular risk profile for use in primary care the Framingham heart study *Circulation* **117** 743–53
- Ecabert O et al 2008 Automatic model-based segmentation of the heart in CT images *IEEE Trans. Med. Imaging* **27** 1189–201
- Haak A et al 2015 Segmentation of multiple heart cavities in 3-D transesophageal ultrasound images *IEEE Trans. Ultrason. Ferroelectr. Freq. Control* **62** 1179–89
- Heusch G, Libby P, Gersh B, Yellon D, Böhm M, Lopaschuk G and Opie L 2014 Cardiovascular remodelling in coronary artery disease and heart failure *The Lancet* **383** 1933–43
- Hoffmann U, Massaro J M, D'Agostino R B, Kathiresan S, Fox C S and O'Donnell C J 2016 Cardiovascular event prediction and risk reclassification by coronary, aortic, and valvular calcification in the Framingham heart study *J. Am. Heart Assoc.* **5** e003144
- Hofman A et al 2013 The Rotterdam study: 2014 objectives and design update *Eur. J. Epidemiology* **28** 889–926
- Iglesias J E and Sabuncu M R 2015 Multi-atlas segmentation of biomedical images: a survey *Med. Image Anal.* **24** 205–19
- Işgum I, Staring M, Rutten A, Prokop M, Viergever M A and Van Ginneken B 2009 Multi-atlas-based segmentation with local decision fusion application to cardiac and aortic segmentation in CT scans *IEEE Trans. Med. Imaging* **28** 1000–10
- Kang D, Woo J, Slomka P J, Dey D, Germano G and Kuo C C J 2012 Heart chambers and whole heart segmentation techniques: review *J. Electron. Imaging* **21** 010901–1
- Kirişli H et al 2010 Evaluation of a multi-atlas based method for segmentation of cardiac CTA data: a large-scale, multicenter, and multivendor study *Med. Phys.* **37** 6279–91
- Klein S, Pluim J P, Staring M and Viergever M A 2009 Adaptive stochastic gradient descent optimisation for image registration *Int. J. Comput. Vis.* **81** 227–39
- Klein S, Staring M, Murphy K, Viergever M A and Pluim J P 2010 Elastix: a toolbox for intensity-based medical image registration *IEEE Trans. Med. Imaging* **29** 196–205
- Lam L and Suen C Y 1997 Application of majority voting to pattern recognition: an analysis of its behavior and performance *IEEE Trans. Syst. Man Cybern. Part A* **27** 553–68
- Lloyd-Jones D M, Larson M G, Leip E P, Beiser A, D'Agostino R B, Kannel W B, Murabito J M, Vasan R S, Benjamin E J and Levy D 2002 Lifetime risk for developing congestive heart failure the Framingham heart study *Circulation* **106** 3068–72
- Lorenz C and von Berg J 2006 A comprehensive shape model of the heart *Med. Image Anal.* **10** 657–70
- Mattes D, Haynor D R, Vesselle H, Lewellen T K and Eubank W 2003 PET-CT image registration in the chest using free-form deformations *IEEE Trans. Med. Imaging* **22** 120–8
- Mozaffarian D et al 2016 Executive summary: heart disease and stroke statistics-2016 update: a report from the American Heart Association *Circulation* **133** 447
- Robertson J, McElduff P, Pearson S A, Henry D A, Inder K J and Attia J R 2012 The health services burden of heart failure: an analysis using linked population health data-sets *BMC Health Serv. Res.* **12** 1
- Rohlfing T, Brandt R, Menzel R, Russakoff D B and Maurer C R Jr 2005 Quo vadis, atlas-based segmentation? *Handbook of Biomedical Image Analysis* (Berlin: Springer) pp 435–86
- Rohlfing T, Russakoff D B and Maurer C R Jr 2004 Performance-based classifier combination in atlas-based image segmentation using expectation-maximization parameter estimation *IEEE Trans. Med. Imaging* **23** 983–94
- Schocken D D, Benjamin E J, Fonarow G C, Krumholz H M, Levy D, Mensah G A, Narula J, Shor E S, Young J B and Hong Y 2008 Prevention of heart failure a scientific statement from the American Heart Association councils on epidemiology and prevention, clinical cardiology, cardiovascular nursing, and high blood pressure research; quality of care and outcomes research interdisciplinary working group; and functional genomics and translational biology interdisciplinary working group *Circulation* **117** 2544–65
- Shahzad R et al 2013 Automatic quantification of epicardial fat volume on non-enhanced cardiac CT scans using a multi-atlas segmentation approach *Med. Phys.* **40** 091910

- Suri J, Wilson D and Laxminarayan S 2007 *Handbook of Biomedical Image Analysis: Registration Models* vol 3 (Berlin: Springer)
- Tavard F, Simon A, Leclercq C, Donal E, Hernández A I and Garreau M 2014 Multimodal registration and data fusion for cardiac resynchronization therapy optimization *IEEE Trans. Med. Imaging* **33** 1363–72
- van Rikxoort E M, Isgum I, Arzhaeva Y, Staring M, Klein S, Viergever M A, Pluim J P and van Ginneken B 2010 Adaptive local multi-atlas segmentation: application to the heart and the caudate nucleus *Med. Image Anal.* **14** 39–49
- Yancy C W *et al* 2013 2013 ACCF/AHA guideline for the management of heart failure: a report of the American College of Cardiology Foundation/American Heart Association Task Force on Practice Guidelines, *J. Am. College Cardiol.* **62** e147–239
- Zheng Y, Barbu A, Georgescu B, Scheuering M and Comaniciu D 2008 Four-chamber heart modeling and automatic segmentation for 3-D cardiac CT volumes using marginal space learning and steerable features *IEEE Trans. Med. Imaging* **27** 1668–81
- Zhuang X, Bai W, Song J, Zhan S, Qian X, Shi W, Lian Y and Rueckert D 2015 Multiatlas whole heart segmentation of CT data using conditional entropy for atlas ranking and selection *Med. Phys.* **42** 3822–33
- Zhuang X and Shen J 2016 Multi-scale patch and multi-modality atlases for whole heart segmentation of MRI *Med. Image Anal.* **31** 77–87
- Zuluaga M A, Cardoso M J, Modat M and Ourselin S 2013 Multi-atlas propagation whole heart segmentation from MRI and CTA using a local normalised correlation coefficient criterion *Functional Imaging and Modeling of the Heart* (Berlin: Springer) pp 174–81